Journal Pre-proofs

Enhanced photosynthetic carbon fixation in microalgae through tandem synergies in electron transport flows

Futao Yi, Libin Yang, Lingjie Zhang, Bo-yu Peng, Xiaobo Tan, Yongyuan Hong, Xiaogang You, Xuefei Zhou, Yalei Zhang

PII: S1385-8947(25)03331-5
DOI: https://doi.org/10.1016/j.cej.2025.162505
Reference: CEJ 162505

To appear in: *Chemical Engineering Journal*

Received Date: 5 February 2025
Revised Date: 29 March 2025
Accepted Date: 8 April 2025

Please cite this article as: F. Yi, L. Yang, L. Zhang, B-y. Peng, X. Tan, Y. Hong, X. You, X. Zhou, Y. Zhang, Enhanced photosynthetic carbon fixation in microalgae through tandem synergies in electron transport flows, *Chemical Engineering Journal* (2025), doi: https://doi.org/10.1016/j.cej.2025.162505

Enhanced photosynthetic carbon fixation in microalgae through tandem synergies in electron transport flows

Futao Yi[1], Libin Yang[1, 2, *], Lingjie Zhang[4], Bo-yu Peng[1], Xiaobo Tan[3], Yongyuan Hong[1], Xiaogang You[1], Xuefei Zhou[1, 2], Yalei Zhang[1, 2, *]

1. *College of Environmental Science and Engineering, Tongji University, Shanghai 200092, China*
2. *State Key Laboratory of Water Pollution Control and Green Resource Recycling, Shanghai Institute of Pollution Control and Ecological Security, Tongji University, Shanghai 200092, China*
3. *School of Chemical and Environmental Engineering, Hunan Institute of Technology, Hengyang 421000, China*
4. *Facultad de Ciencias, Universidad Autonoma de San Luis Potosi, Av. Parque Chapultepec 1570, San Luis Potosi 78210, Mexico*

[*]To whom correspondence should be addressed. Tel: +86-21-65985811; Fax: +86-21-65985811. E-mail: neuqyanglibin@126.com (Libin Yang), zhangyalei@tongji.edu.cn (Yalei Zhang).

Abstract

Excessive CO_2 from human activities was released into atmosphere, resulting into global climate change. Microalgae play a significant role in carbon sequestration, whereas the low quantum efficiency during photosynthesis limits the application of microalgae cultivation in plant carbon fixation and sustainable solar energy conversion. In this study, the mixture containing red and blue fluorescent carbon quantum dots were utilized to enhance microalgal carbon fixation due to their tandem synergies both *in vivo* and *in vitro*. The biohybrid system demonstrated a 1.8-fold increase in carbon fixation and a 1.6-fold increase in energy storage capability. The improved extracellular conductivity and enhanced anaerobic photosynthesis indicated that extracellular electrons are internalized into intracellular photosystem II (PS-II). Furthermore, reduced oxidative stress and an optimized ratio of photosystem I/II activity (~1.6) confirmed the synergy of electron transfer from PS-II to PS-I. Specifically, the CQDs facilitated efficient electron transport along the entire electron transport chain, enhancing both extracellular electron uptake and intracellular electron flow between PS-II and PS-I. This study represents the first instance of enhancing photosynthetic carbon fixation in microalgae through tandem synergies along the entire electron transport chain. These findings offer a novel approach for carbon recycling and sustainable energy generation via photosynthesis, providing valuable insights for the rational design of conductive nanomaterials aimed at activating photosynthetic electrons for both extracellular and intracellular processes.

Keywords

Photosynthetic carbon fixation, Bioelectric conduction, Microalgae, Carbon quantum dots, Linear electron flow

1. Introduction

Over the past decade, approximately 18.7 billion tons of CO_2 have been released into atmosphere annually, significantly contributing to the intensifying greenhouse effect. [1] Photosynthesis is the dominate metabolic process through which green plants and cyanobacteria fix carbon dioxide and water to synthesize carbohydrates, powered by sunlight. [2] Among various photosynthetic organisms, microalgae are particularly noteworthy, contributing over 50% of the global carbon fixation efficiency in plant while also converting carbon dioxide into valuable chemicals such as antibiotics, proteins and lipids etc. [3] However, the low efficiency of solar-to-biomass energy conversion in microalgae has primarily limited their overall photosynthetic efficiency. [4] The core of photosynthesis lies in converting solar energy into chemical energy through electron flow, yet microalgae exhibit a low electron flow efficiency of merely 4%, severely limits their capacity for carbon fixation. [5, 6] Much efforts were attempted to activate the photosynthetic efficiency in microalgae, such as the regulation of light wavelength [7] and co-culture with other microorganism. [8] The first method might activate pigments in photosystems, whereas the activation difference might result into photo protection to limit the algal photosynthesis. The latter strategy might develop the algal photosynthesis by the mutualism process. However, the introduction of other microorganism might result the nutrition competition to inactivate microalgae.

During photosynthetic electron flow, extracellular electrons can be transformed into intercellular photosystem (PS) via transmembrane transport and linear electron flow (LEF). In the research of algae-supported microbial fuel cells, microalgae were utilized as the electron transport medium between cathode and anode chamber. This independent unit should transfer electrons in the microalgae species. [9] Enhancing microalgal carbon fixation by suppling additional active electrons suggests the potential of utilizing extracellular electrons within intracellular PS-II. [10] Extracellular electrons from electroactivity extracellular polymeric substances (EPS) may be carried into intracellular PS-II by binding proteins and proper potential effect. [11] These extracellular electron transfer (EET) processes can provide more excited electrons for Calvin cycle, thereby enhancing carbon fixation. Efforts have also been made to improve conductivity in PS-I or II, aiming to enhance LEF electron transport from PS-II to PS-I. Activation of PS-II via blue light regulation, coupled with enhanced electron transport, can assist the Hill reaction, providing additional active electrons to support carbon fixation.[12] Similarly, red florescent semiconductors have been shown to increase electron excitation in PS-I, generating NAPDH to supply sufficient energy for LEF. [13] However, most research has focused on the activation of single PS, often leading to the imbalanced reactions. Overexcitation of electrons within the photosystems can overload the electron chain, potentially generating reactive oxygen species (ROS) in respiratory chain, which can damage microalgae. [14] Given the complexity of the entire photosynthetic process, researched have long grappled with the challenge of regulating and activating the entire

electron chain in a tandem manner.

Strategies that activate extracellular-intracellular electron transfer and optimize intracellular PS enhancement hold significant promise for boosting microalgal photosynthesis. Nanomaterials, in particular, may facilitate electron conductivity for electrons transfer. Additionally, the intracellular Emerson effect suggests the influence of light spectra and phototropism on photosynthesis, where multi-colored light enhances the activity ratios of PS-I and PS-II. [7, 15] Therefore, tandem synergies at both the extracellular and intracellular levels require the incorporation of low-toxic, conductive, and fluorescence-controllable nanomaterials into microalgae cultivations. Non-metallic carbon quantum dots (CQDs) are highly advantageous in biological systems due to their low toxicity and excellent bioavailability. [16] Unique structure in carbon quantum dots (CQDs) provides notable conductivity, making them suitable for applications in bioelectronics and biosensors. Furthermore, their fluorescence properties can be tuned via surface modifications, potentially enhancing photosynthesis through the multi-excitation in chlorophyll. [17] These characteristics make CQDs ideal candidates for improving photosynthesis efficiency through tandem synergies. Previous studies have confirmed that CQDs from antibiotics and citric acid can enhance microalgal photosynthesis by activating extracellular or intracellular electron transfer pathways. [18-20] However, the potential for CQDs to synergistically enhance the entire electron flow remains underexplores. This limitation could potentially constrain the comprehensive understanding of the photosynthetic mechanism and hinder the rational design of more effective enhancement strategies.

In this study, the carbon fixation performance of microalgae was significantly enhanced by incorporating mixed carbon quantum dots (CQDs) containing red and blue emission into the cultivation medium. This research represents the first attempt to augment microalgal photosynthetic activity through tandem synergies, focusing on enhanced extracellular-intracellular electron transfer and balanced activation of two intracellular photosystems across the entire electron transport chain. Photosynthetic performance was systematically evaluated by measuring carbon fixation rates and the relative activities of key enzymes. Furthermore, we demonstrated the intracellular utilization of extracellular electrons in photosynthesis through anaerobic photosynthesis assays and photoelectric experiments. The balance between photosystems was quantitatively confirmed by analyzing the active sites of each photosystem and monitoring LEF. Notably, the optimized ratio of PS-I/PS-II activity (~1.6) and reduced oxidative stress highlighted the synergistic electron transfer from PS-II to PS-I, which was facilitated by the CQDs. This study provides a novel approach to advancing carbon neutrality and sustainable energy production by integrating functional nanomaterials with photosynthetic organisms. The findings offer valuable insights into the rational design of conductive nanomaterials for enhancing both extracellular and intracellular electron transport in photosynthesis.

2. Materials and Methods

2.1 Microalgae culture

The photosynthetic microalgae species, *C. pyrenoidosa* (strain No. FACHB-9) and *Tetradesmus obliquus* (strain No. FACHB-12) were obtained from the Institute of Wuhan Aquabiology of the Chinese Academy of Sciences, China. The microalgal cultivation process followed the same protocol as described in our previous study research. [16, 21, 22] According to prior engineering research, which identified the optimal conditions for carbon fixation efficiency, *C. pyrenoidosa* was inoculated at an initial concentration of 1×10^6 cells/mL in each experimental group.

Multicolor carbon quantum dots (CQDs), including blue (B-), green (G-), yellow (Y-), red (R-), and a red-blue composition (B+R) at a 4:1 ratio, were used in this study. The composite ratio followed with previous research in monochromatic light-emitting diodes to enhance microalgal growth and biodiesel production. [23] All CQDs were prepared at a concentration of 10 mg/L. The CQDs were dispersed into the culture medium using ultrasound, and the resulting suspension was mixed with air bubbling throughout the cultivation period. The preparation and characterization of the CQDs are detailed in Supporting Information **Text S1**. Considering to enhance the conductivity of CQDs, the nitrogen-doping was utilized to modify CQDs. [24]

2.2 Cell density and determination of intracellular composition in microalgae

To evaluate the culture efficiency under different conditions, microalgae cells were counted using a flow cytometer (FACScalibur, Becton Dickinson, USA). During the 10-day cultivation period, 2 mL of the algae culture was collected daily for cell counting and observation. The specific growth rate (M), used as a parameter to evaluate microalgae growth, was calculated using the following equation:

$$M=\frac{\ln(N_t-N_{t-\Delta t})}{\Delta t} \quad (1)$$

where N_t and $N_{t-\Delta t}$ were cell density in the time t and $t-\Delta t$. Moreover, Δt was the time interval between above two tests.

Detection methods of intracellular substance such as chlorophyll, protein, carbohydrate, and lipid were all illustrated at **Text S2**.

2.3 Carbon fixation and energy storing calculation from microalgal photosynthesis

The carbon fixation efficiency of microalgal photosynthesis were counted by the total organic carbon content in biomass ($E_{C\text{-}biomass}$) and EPS ($E_{C\text{-}EPS}$), the related content was measured by total organic carbon analyzer (Shimazu, Japan). The equation for total carbon fixation efficiency ($E_{c\text{-}total}$) was proved as follow:

$$E_{C\text{-}total}=E_{C\text{-}biomass}+E_{C\text{-}EPS} \quad (2)$$

According to our previous research, the major components of microalgae cells were carbohydrate, lipid, and protein. The amount of energy produced for complete oxidation was 15.7 KJ/g for carbohydrate, 37.6 KJ/g for lipid, and 16.7 KJ/g for protein. [25] Thus, the biomass energy of microalgae was derived from the following equation:

$$\text{Biomass Energy (kJ)} = \text{Dry Weight (g)} \times [\text{Carbohydrate Content (\%)} \times 16.7\text{kJ/g} + \text{Lipid Content (\%)} \times 36.7\text{kJ/g} + \text{Protein Content (\%)} \times 16.7\text{kJ/g}] \quad (3)$$

2.4 Extracellular electron transform validation

Photo-current response and electrochemical impedance spectroscopy (EIS) were utilized to measure the conductivity of microalgae-CQD composites. [19] In these experiments, the composite and individual microalgae served as working electrodes, while a platinum electrode and an Ag/AgCl electrode were used as the counter and reference electrodes, respectively. During the photo-current response measurements, current intensity was monitored through light-dark cycles (20s-20s). The $Fe(CN)_6^{3-}$ solution (2M) was employed as the electrolyte, with an operating voltage of 2V for the EIS scanning. The extracellular electron transform was also validated by the anaerobic photosynthesis experiment, the detail was proved in **Text S3**.

2.5 Total photosynthetic activity measurement

The total photosynthetic activity was assessed through multi-enzyme quantification and product analysis. $NADP^+$/NAPDH and ADP/ATP concentrations, along with ATP synthase activities in various biohybrid systems, were determined following the methodologies of Huang and Cruz in **Text S4**. [19, 26] The RuBisCo content was tested as followed by the Ellisa Assay Kit (Shanghai ruifan Biological Technology Co,Ltd) and the details were enlisted at **Text S5**.

2.6 Photosystem I/II activity

PS-I activity was assessed using an Fe-S protein assay kit and a chlorophyll fluorescence meter (PAM-100, Walz). The PS-II activity was determined by measuring oxygen evolution with a Clark-type oxygen electrode; specific test procedures are detailed in the Supplementary Information. [19] Additionally, the chlorophyll fluorescence meter was employed for evaluating PS-II activity. The P515 signal method was used to quantify the number of active PS-I and PS-II sites in microalgae. [27]

2.7 Analysis of photo-protection stress and electron transportation between PS-I/II

Characteristic substances of oxidative stress, including intracellular reactive oxygen species

(ROS), superoxide dismutase (SOD), and malondialdehyde (MDA), were quantified using corresponding assay kits (Jiancheng Bioengineering Institute, Nanjing, China) in **Text S6**. The non-photochemical quenching (NPQ) index, a crucial metric for demonstrating active electron quenching and self-oxidation in PS-II, was measured using a chlorophyll fluorescence meter. Additionally, the efficiency of electron transfer between PS-I and PS-II was assessed using 77K fluorescence spectra (**Text S7)**. [28]

3. Result and Discussion

3.1 Characterization of CQDs

Several characterizations confirmed the presence of CQDs and delineated their optic-electric attributes. HRTEM images revealed that the CQDs exhibited nanosphere morphologies and displayed the (002) plane characteristic of graphite layers (**Figure 1a** and **1b**), indicating successful synthesis. The CQDs with different size (~5nm for RCQDs and ~3nm for BCQDs in **Fig. S1**) interacted obviously and it supported the heterojunction between BCQDs and RCQDs could be confirmed. In the realm of optical and energy capture, the absorption peaks in the blue and red regions for microalgae are associated with Soret and Qy transition bands of chlorophyll. (See in **Figure 1c**) [29] The emission spectra of B- and R-CQDs significantly overlap with the absorption spectrum of the microalgae, suggesting a potential for efficient energy transfer in the photosynthesis. This phenomenon suggested the dual excitation in chlorophyll, which indicated that the synergistic effect of blue and red emissions enhances quantum efficiency in microalgal carbon fixation.

The optical and structural properties of CQDs were hypothesized to influence their fluorescence and conductivity, which could affect the photosynthetic process in microalgae. The band edges for various CQD samples were situated at 494 nm, 533 nm, 632 nm, and 692 nm, corresponding to B-CQDs, Y-CQDs, G-CQDs, and RCQDs, respectively (**Figure 1d)**. Using an empirical equation, the band gaps of these samples were calculated, revealing a progressive decrease from 2.51 eV to 1.79 eV. The reduction of band gap is inversely related to particle size and the number of graphite layers, because of the quantum confinement effect. [30] This hypothesis is further supported by the particle size differences observed in **Figure S2**. The observed redshift in the band edges, along with the narrower band gaps, indicates enhanced light absorption and electron excitation capabilities.

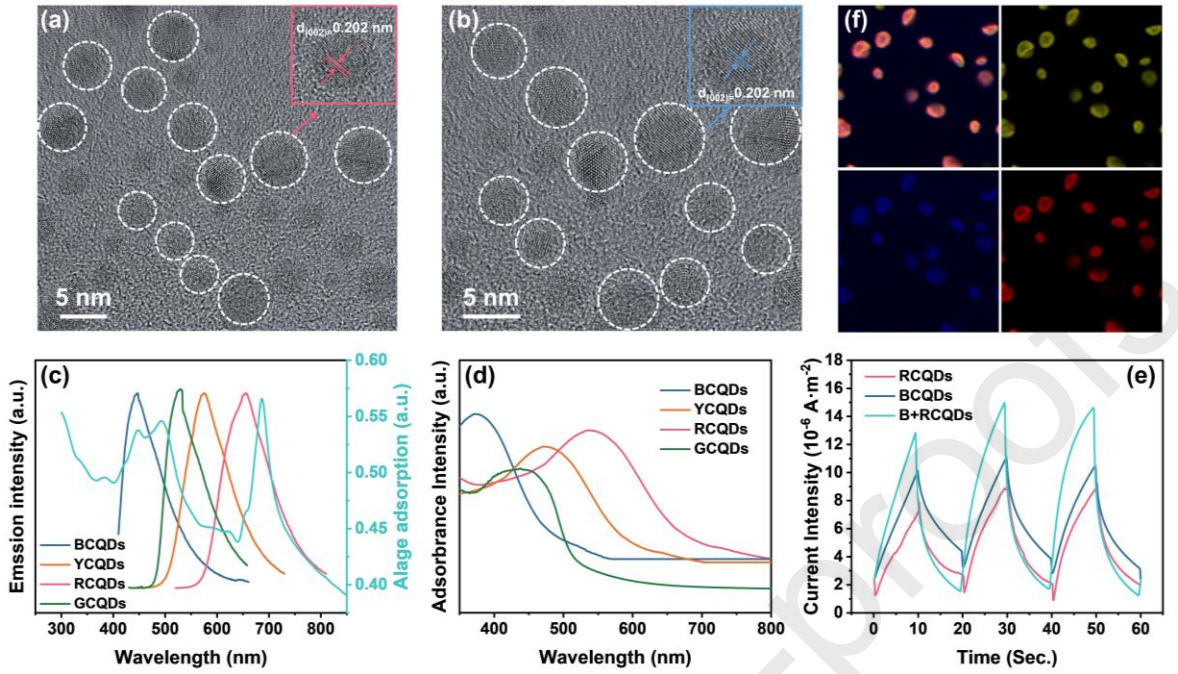

Figure 1 Characterization of CQDs. TEM imagines of (a) BCQDs and (b) RCQDs with its (002) plan lattice distance, (c) Florescent spectra of CQDs with the excitation of 420nm and absorption of *C. pyrenoidosa*, (d) UV-vis absorption spectra of all CQDs samples in 350-800nm range, (e) photo-current response of different CQDs samples in mixed 0.1M $Fe(CN)_6^{3-}$ and 0.1M PBS solution (100mg biohybrid in each electrode), (f) CLSM images of overlap, microalgae cells, BCQDs, and RCQDs ex wavelength: 488 nm and emission wavelength:450-780nm in the microalgae with B+RCQDs cultivation (2mL microalgae solution for scanning microscopy).

Additionally, the B+RCQDs electrode demonstrated the highest photocurrent intensity (See in **Figures 1e** and **S3**), suggesting superior conductivity among the CQD samples. [31] The slow decay of current from B+RCQDs electrode also suggested the BCQD/RCQD heterojunction should save electrons for the latter utilization, this continuous recession could be attributed into the rich conjunction structure in the composite CQDs to attract electrons. [32] This composite heterojunction may facilitate accelerated intracellular and extracellular electron transport, offering broad implications for various biological applications. Taken together, characterizations substantiated the successful fabrication of multicolor fluorescent CQDs. The composite B+R-fluorescent CQDs, with their enhanced light absorption and conductivity, are posited to bolster the transformation of photo-electric energy during the microalgal carbon fixation. [33]

The interaction between CQDs and microalgae cells was elucidated using confocal laser scanning microscopy (CLSM). **Figure 1f** displays the colocalization of three distinct colors—red

for RCQDs, blue for BCQDs, and yellow for microalgae cells. This colocalization indicates that BCQDs and RCQDs are present both inside and outside the cell walls of *C. pyrenoidosa*. This distribution may influence the microalgae's photosynthetic CO_2 fixation and overall growth.

3.2 Photosynthetic CO_2 fixation and growth of microalgae interacted by CQDs

The growth of *C. pyrenoidosa* was significantly enhanced by the addition of various fluorescent CQDs in **Figure 2a** and **S4**. Compared to the blank, all types of CQDs promoted microalgae growth, with the enhancement order being Blank < GCQD < YCQD < RCQD < BCQD < B+RCQD. The same enhanced trend and order also could be confirmed into *Tetradesmus obliquus* cultivation (**Fig. S5**). Notably, cultivation with B+RCQDs (10 mg/L) resulted in the highest cell density 199.26 (± 6.87) $\times 10^6$ cells/mL (**Fig. S4**), surpassing single B- and R-CQDs by factors of 1.22 and 1.45, respectively. Moreover, in the B+RCQDs with different concentrations, 10mg/L proved the best efficiency in the microalgae cultivation, which was much lower than other analogous research, the relative low concentration of CQDs could reduce environmental toxicity and risk. [19, 34] The maximum specific growth rate (μ_{max}) in **Figure S6** corroborates this enhancement, with B+RCQDs showing an 18.70% increase over the blank. This stimulation may be attributed to the increased intracellular and extracellular electron flux, resulting the metabolic activation. [35, 36] Efficient electron transportation supports photosynthesis and Calvin-Benson-Bassham (CBB) cycle, potentially generating more energy precursors, such as NADPH, ATP, and proteins. [37] The composite B+R-CQDs, with their dual fluorescence, may induce the dual excitation in chlorophyll, activating photosystems and carbon fixation, thereby accelerating intracellular electron transport and metabolism.

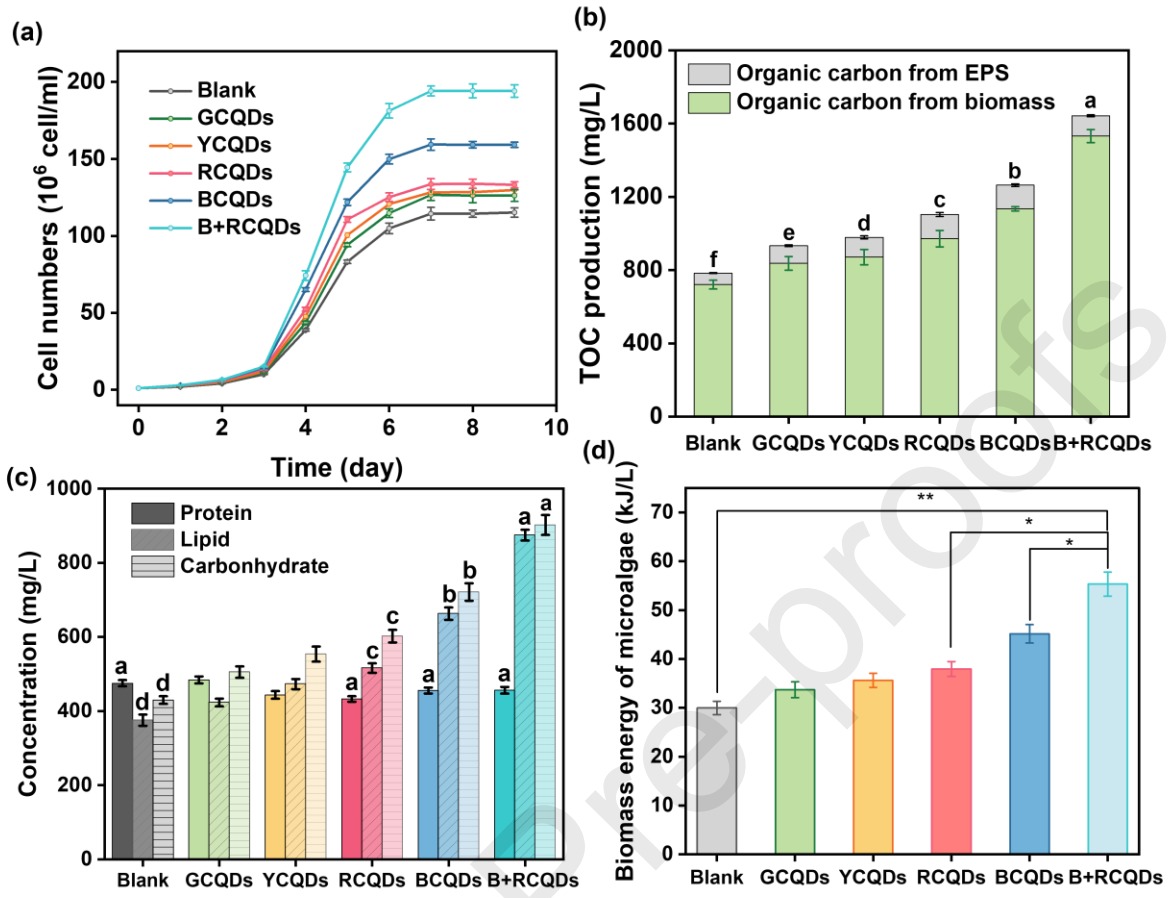

Figure 2 The effect of CQDs to microalgal growth and carbon fixation. (a) microalgal cell density in different CQDs cultivation (The CQDs concentration was 10mg/L), (b) organic carbon content in microalgae biomass and EPS within different CQDs addition, (c) product concentration from the microalgal carbon fixation and (d) related biomass energy from microalgal carbon fixation product (P<0.05, n=3).

The photosynthetic CO_2 fixation performance showed a total organic carbon increasement within both biomass and EPS from microalgae cultivated with CQDs (**Figure 2b**). Among various CQDs, B+RCQDs exhibited the highest activity in $E_{C\text{-}total}$ (1643.60 ± 33.40 mg·L^{-1}), representing a 29.98% and 67.82% improvement compared to single B (1264.63 ± 40.30 mg·L^{-1}) and RCQDs (979.35 ± 32.57 mg·L^{-1}). The fixation trends paralleled the cultivation ranking, suggesting a positive correlation between microalgae growth and photosynthetic CO_2 fixation. [38] Although CQDs cannot be separation from samples TOC measurement, its low concentration (10mg • L^{-1}) in the algae cultivation suggested its negligible role in the test, comparing to the high TOC concentration in each sample. Deeply, CQDs cultivation led the more organic carbon content in EPS, which indicated the more active CO_2 fixation to secrete extra organic compounds into

extracellular. Furthermore, comparing into single florescent BCQDs (129.74 ± 8.73 $mg \cdot L^{-1}$) and R-CQDs (132.55 ± 6.57 $mg \cdot L^{-1}$), B+RCQDs cultivation (111.10 ± 9.33 $mg \cdot L^{-1}$) proved less EPS production. (**Figure S7)** This trend may signal less peroxidation stress to benefit photosynthesis from dual florescent CQDs. [39]

In terms of biomass, EC-biomass cultivation showed significantly higher total carbon fixation than B- and R-CQDs, with concentrations at 1532.50 ± 27.73 $mg \cdot L^{-1}$, 1.36 and 1.56 times greater, respectively. Organic carbon content correlated positively with cell density, as organic compounds such as lipids, proteins, and polysaccharides constitute the primary framework of microalgae cells. [40] Consequently, active organic synthesis through the ATP consumption contributed to the high organic carbon content in biomass, indicating efficient electron transfer facilitated by CQDs additions. [41] Efficient cell proliferation and more organic carbon content in biomass both present more CO_2 fixation activity from the B+RCQDs cultivation. Based on biomass and EPS calculation, it further illustrated the more active photosynthetic performance from composite B+RCQDs activation. These improvements in microalgal carbon fixation performance show promise for greenhouse gas mitigation.

3.3 Intracellular substances and energy storing calculation from microalgal photosynthesis

Intracellular substances, such as carbohydrates, lipids and proteins, were products of microalgal photosynthesis, with their content linked to carbon fixation and energy storage processes. The CQDs/microalgae biohybrid system enhanced carbohydrates generation could be confirmed in **Figure S8a**. Specifically, systems with RCQDs, BCQDs, and B+RCQDs showed significantly higher carbohydrate content compared to the blank ($P < 0.05$). Carbohydrates, as products of CO_2 fixation, indicate the activity of photosynthesis and electron transport in the C3 and CBB cycles. Their concentration correlates positively with microalgal photosynthetic activity and increased carbohydrate production from the B+RCQDs biohybrid suggested enhanced photosynthetic and electron transport activities. [42] Moreover, lipid and proteins are other product of carbon fixation by energy conversion (**Figure 2c**), further indicating enhanced photosynthesis. The surplus carbohydrates from active photosynthesis promote lipid accumulation through activation of the tricarboxylic acid cycle. [43] These high levels of intracellular substances observed underscore active carbon resource utilization by microalgal photosynthesis in biohybrids.

The intracellular substances present in these products serve as ideal bioenergy sources and valuable chemicals, energy storage within these products was quantified using microalgae components. Owing to the intracellular substance improvement within CQDs addition, the energy stocking in microalgal biomass was also developed. (See in **Figure 2d**) Among various cultivation conditions, the B+RCQDs addition proved the most energy storage in microalgae components (55.33 ± 2.45 kJ). The enhanced lipid accumulation and nutrients uptake from CQDs additions was the main reason for the obvious energy stocking. [44] Comparing to the other cultivation condition, B+RCQDs showed increases of 86.28%, 45.83%, and 22.59% relative to blank, RCQDs,

and BCQDs, respectively. The biohybrid composites of CQDs integrated with active photosynthesis demonstrated potent energy storage via carbon fixation into organic chemicals. This method presented a green and effective approach for sustainable carbon treatment and chemical production.

3.4 Enzymes and intermediates analysis for the microalgae photosynthetic activation

The enhancement of photosynthetic activity in microalgae using B+RCQDs was investigated by assessing key enzymes and metabolites involved in the C3 photosynthetic cycle. [45] The activity of RuBisCo, a crucial enzyme in converting CO_2 to C3 carbohydrates, was highest in microalgae cultivated with B+RCQDs compared to other treatments (**Figure 3a**). This elevated RuBisCo activity suggested a metabolic activation effect exerted by B+RCQDs, consist with the observed enhancement in photosynthetic carbon fixation. Previous studies have indicated that the increased electron conductivity can stimulate RuBisCo activase, which was modulated by ATP generated in the electron transport chain. [46] In our study, the heightened activity observed in B+RCQDs-cultivated microalgae could be attributed to improved electron transport, potentially induced by the composite nature of CQDs. This active metabolism is further supported by increased concentration of carbohydrates and the efficient conversion of inorganic carbon in B+RCQDs cultivation. The active RuBisCo enzymes underscored the effective conversion of light energy into chemical energy stored in organic compounds.

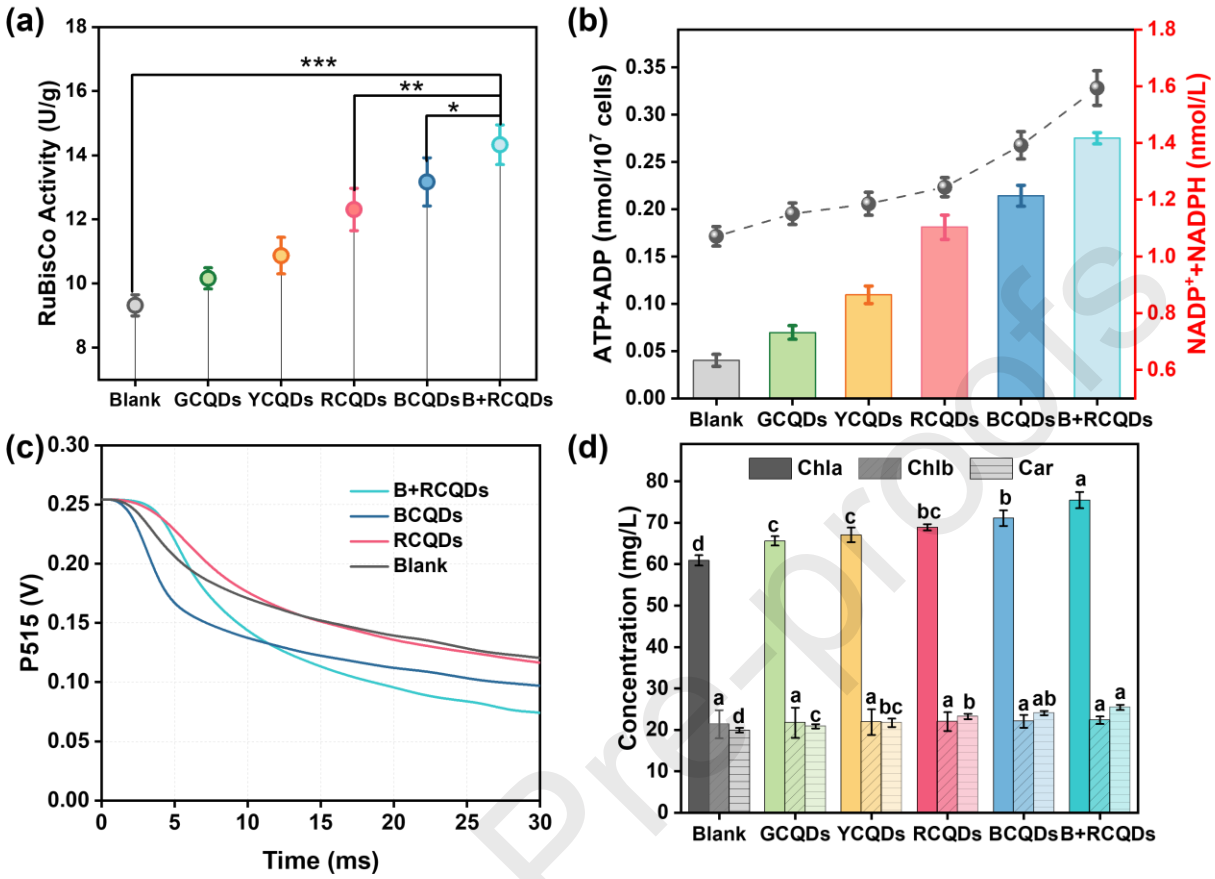

Figure 3 Enzymes and intermediates analysis for the microalgae photosynthetic activation. (a) RuBisCo content in microalgae with different CQDs cultivation in BG-11 medium, 1mL biohybrids in each test (n=3, *P*<0.05). (b) ATP/ADP and NADP$^+$/NADPH content in different biohybrid, 0.5mL biohybrids in each test (n=3, *P*<0.05), (c) activity measurement of ATP syntheses, the half-decay time could be regarded as the activity of ATP syntheses, (d) pigment in in different biohybrid (Chl a, chlorophyll a; Chl b, chlorophyll b; Car, carotenoid).

To substantiate the role of photosynthetic energy and electron carriers in this enhancement, we conducted a 14-day quantification study. The B+RCQDs treatment exhibited the highest levels of energy carriers, showing 1.9 and 2.2-fold increase in ATP/ADP and NADP$^+$/NADPH contents, respectively, compared to the control group (**Figure 3b**). The enhanced energy carriers suggested that more light energy injected into electron transform in CBB cycle and carbon fixation by the B+RCQDs cultivation. [47, 48] The positive effect for the microalgal carbon fixation was also proved in other red florescent nanomaterials via the PS-I activation. [49] Moreover, real-time PCR and metabonomic analysis in our previous research and other reports, carbon based-QDs addition in the microalgae cultivation might activate the metabolism in carbon fixation and fatty acid

metabolism. These enhancements both beneficial for carbon fixation to accumulate more organic carbon into lipids. [16, 50] It was likely facilitated by electron and proton transportation from the conductive CQDs (**Figure S8**). [51] Moreover, the accelerated electron transport likely influenced ATP synthase activity by P515 measurements, supporting the enhanced conductivity in the biohybrid system (**Figure 3c**). The H^+ conductivity in the B+RCQDs biohybrid (11.92 s^{-1}) was superior to that in B- (13.12 s^{-1}) and R- (23.43 s^{-1}) CQDs treatments, indicating the most efficient ATP synthesis in the B+RCQDs biohybrid. [52] The activation of ATP synthesis is connected to mitochondrial proteins involved in glucose and lipid metabolism, it was stimulated by active electron transformation in the mitochondria. [53] Owing to its ideal conductivity, the intracellular CQDs might act as carriers to shuttle electrons in the mitochondria. The active generation of ATP and NADPH in the B+RCQDs treatment confirms effective energy and electron transformation in the photosynthetic carbon fixation.

Pigments such as chlorophylls and carotenoids, serving as major antenna molecules for light energy absorption and photosynthetic electron excitation, were evaluated. After 14 days of cultivation, the B+RCQDs biohybrid exhibited significantly higher chlorophyll a content ($P < 0.05$), indicating improved light absorption for photosynthetic electron excitation (**Figure 3d**). The red and blue fluorescence emitted by the CQDs may regulate the synthesis of chlorophyll a (Chl a), influenced by the light-harvesting capabilities of the microalgae. Additionally, the addition of composite CQDs improved the chl a/b ratio, suggesting enhanced PS-I activity and electron transport efficiency compared to single CQDs treatments. [54] (**Figure S9**) In the photosynthetic LEF, Chl a excites the light-harvesting complex I (LHC-I) in PS-I, promoting electron transport and energy conversion from PS-II to PS-I through efficient energy capture. [55] The proper activation of PS-I also helps to mitigate photoprotection and activate PS-II, because this process could dephosphorylate in LHC-II. [52] Thereby, B+R-CQDs addition prove the potential to improve both PS-I and II activity in LEF. The B+R-CQDs also induced the highest carotenoid concentration, which was 20.36% greater than that of the control. It further demonstrated that B+R-CQDs may facilitate photosynthetic carbon fixation and intracellular electron transport. Enhanced photosynthetic carbon fixation in B+RCQDs cultivation is corroborated by enzyme and intermediates analysis, confirming efficient electron transport observed.

3.5 Photosynthesis enhancement from synergy of extracellular-intracellular electrons transfer

The role of extracellular electron transfer in the enhancement of photosynthetic carbon fixation by B+RCQDs merits in-depth analysis, given their ability to facilitate extracellular electron transfer at the microalgae cell wall. Applying principles from microbial electrochemistry, we conducted photo-current measurements to evaluate extracellular electron conduction in microalgae. The weak light current intensity (15.32×10^{-7} $A\cdot cm^{-2}$) in the single microalgae electrode substantiated the poor extracellular electron conduction in microalgae. (**Figure 4a** and **S10a**) The increased current intensity in the biohybrid systems suggests superior conductive

properties conferred by the addition of CQDs, especially the highest intensity in the B+RCQDs biohybrid (33.74×10^{-7} $A\cdot cm^{-2}$). Furthermore, reduced arc in electrochemical impedance spectroscopy (EIS) spectra confirms improved extracellular electron conduction in the CQDs biohybrid, with B+RCQDs demonstrating the most significant effect (**Figure 4b** and **S10b**). [56] The active EPS in the biohybrid likely generated electroactive components such as proteins, polysaccharides, and humic acids, which, along with the conductive CQDs, served as electron shuttles in EET. [57] Consequently, the enhanced EET in the B+RCQDs biohybrid was evident, it might provide more active extracellular electron for intracellular carbon fixation.

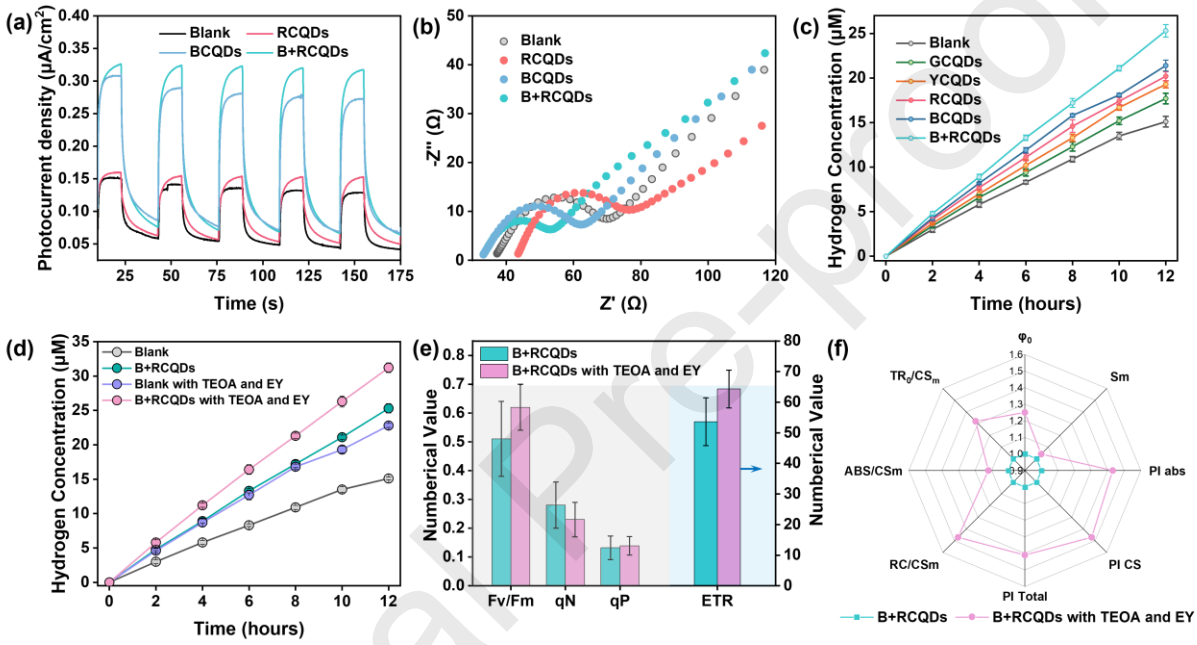

Figure 4 Extracellular-intracellular electrons transfer analysis. (a) Photo-current response and (b) EIS spectra in different biohybrids, photosynthetic HER activity measurement in in mixed 0.1M $Fe(CN)_6^{3-}$ and 0.1M PBS solution, (c) different biohybrids and (d) agents addition (1.5 $mg\cdot L^{-1}$ Eosin Y disodium salt (EY) and 100 $mg\cdot L^{-1}$ triethanolamine (TEOA)), (e) histograms of chlorophyll fluorescence characteristics, (f) Corresponding spider plots of chlorophyll fluorescence parameters from anaerobic PS-II.

Beyond cell-cell transfer, extracellular electrons also penetrate the intracellular metabolic processes. The anaerobic hydrogen evolution reaction (HER) serves as an effective assay for demonstrating the promotional effect of extracellular electrons on photosynthesis. The HER rate in the B+RCQDs biohybrid reached 15.10 μmol H_2 (mg chlorophyll) $^{-1}\cdot h^{-1}$, marking a significant enhancement over 3.23 μmol H_2 (mg chlorophyll) $^{-1}\cdot h^{-1}$), R-CQDs (2.51 μmol H_2 (mg chlorophyll) $^{-1}\cdot h^{-1}$) and blank (1.80 μmol H_2 (mg chlorophyll) $^{-1}\cdot h^{-1}$) cultivations (**Figure 4c**). The enhanced HER in biohybrid supported the previous research that extracellular electrons in microalgae could

be involved into intracellular LEF in photosynthetic hydrogen production. [58] All HER results indicated slow EET in the single microalgae and the B+RCQDs could speed up the EET transfer to reinforce the intracellular photosynthetic carbon fixation. Lipids might work as fat-soluble electron shuttles to transform extracellular electrons from outer membrane into macroalgae cells. The intracellular substances measurement validated that the enhanced lipids generation from CQDs might further assist the electron internalization. [59] To further validate the role of extracellular electrons internalization, photosensitizer (EY) and sacrificial agent (TEOA) were employed in the HER with the B+RCQDs biohybrid, resulting in a 23.32% and 34.57% improvement in hydrogen generation efficiency, respectively (**Figure 4d** and **S11**). Moreover, the addition of these two kinds of agent also activated the blank group without any CQDs and it might indicates that the improvement was due to electron transmembrane transport rather than electrons generated by extracellular CQDs. This finding corroborates the promotional effect of the extracellular-intracellular electron transfer in the photosynthesis.

The carbon fixation enhancement from extracellular electrons internalization was further investigated using chlorophyll fluorescence transient curves and kinetic parameters in PS-II under different cultivation conditions. The photochemical quenching coefficient (*qP*) increased by 5.34% with the addition of agents, while the non-photochemical quenching coefficient (*qNP*) decreased by 34.60%, indicating a higher energy consumption in intracellular PS (**Figure 4e**). [49] In the energy utilization side, the elevated quantum yield for electron transport (*Fv/Fm*) and electron transport rate (*ETR*) suggest that more light energy and intracellular electrons are being utilized in the LEF and latter carbon fixation. The chlorophyll fluorescence curve also revealed an increase in maximum chlorophyll fluorescence (*Fm*), indicative of activated D1 protein and a greater capacity for electron acceptance in PS-II. The less energy requirement for complete plastoquinone reduction (*Sm*) provides robust evidence for an expanded PQ pool and efficient electron transformation in the intracellular LEF. [60] All these data both pointed out the effective energy utilization and effective intracellular electron transform from the extracellular electron internalization.

In terms of reaction centers within PS-II, the increased number of PS-II reducing centers per excited cross-section (*RC/CSm*) indicates a higher density of reaction centers. Energy flux analysis in PS-II showed that the absorbed energy (ABS) and trapped energy (TRo) per CS_m also increased with TEOA and EY stimulation. This trend suggested that more photo energy was absorbed and utilized in the LEF to reduce PQ. In details, more energy input could lead into a considerable improvement in absorption (PI_{abs}), cross-section (PI_{cs}), and energy conversion (PI_{total}) performance (**Figure 4f**). [61] The chlorophyll fluorescence data from PS-II illustrated that B+RCQDs expedite the internalization of extracellular electrons into intracellular PS-II, facilitated by their excellent conductivity. These active electrons are subsequently integrated into the LEF, thereby enhancing the transformation and internalization of extracellular electrons. This process provided additional electrons and energy to support intracellular photosynthesis and carbon

fixation.

3.6 Photosynthesis enhancement from synergy of intracellular PS-I/II electrons transfer

Intracellular electron transfer constitutes a crucial step in the internalization of extracellular electrons necessary for completing photosynthetic carbon fixation. The energy requirement for this process is derived from successive electron excitations in PS-II and I. To assess PS-II activity initially, chlorophyll fluorescence parameters were employed (**Figure 5a** and **S12**). The ETR increased with the addition of CQDs, with B+RCQDs showing the highest enhancement, indicated greater energy input and electron conduction for carbon fixation. This increase is attributed to the enhanced electron conduction and light absorbance due to the dual excitation in chlorophyl. Concurrently, the active generation of NADPH provides additional energy for the reduction of the plastoquinone pool and phosphorylation of the D1 protein, a key reaction to activate PS-II. [62] The improved electron and energy transformation in B+RCQDs biohybrids is further evidenced by a significant decrease in photoenergy quenching indices, like m_0 and v_j. It suggested that the B+RCQDs conduct the intracellular electron in PS-II to avoid the quenching effect. The superior intracellular conductive activity of the B+RCQDs biohybrid is corroborated by oxygen evolution measurements in the Hill reaction. (**Figure 5b**) In comparison, BCQDs were found to be more effective in activating PS-II and water splitting than RCQDs, due to the ATP-ADP conversion in biohybrids. [63] Furthermore, the conductive nature of CQDs may also catalyze photophosphorylation and RuBisCo activation, facilitating ATP synthesis and consumption for subsequent energy supply. [64] A series of PS-II measurements indicate that B+RCQDs exhibit the most efficient activation, with a notable activation trend observed for BCQDs.

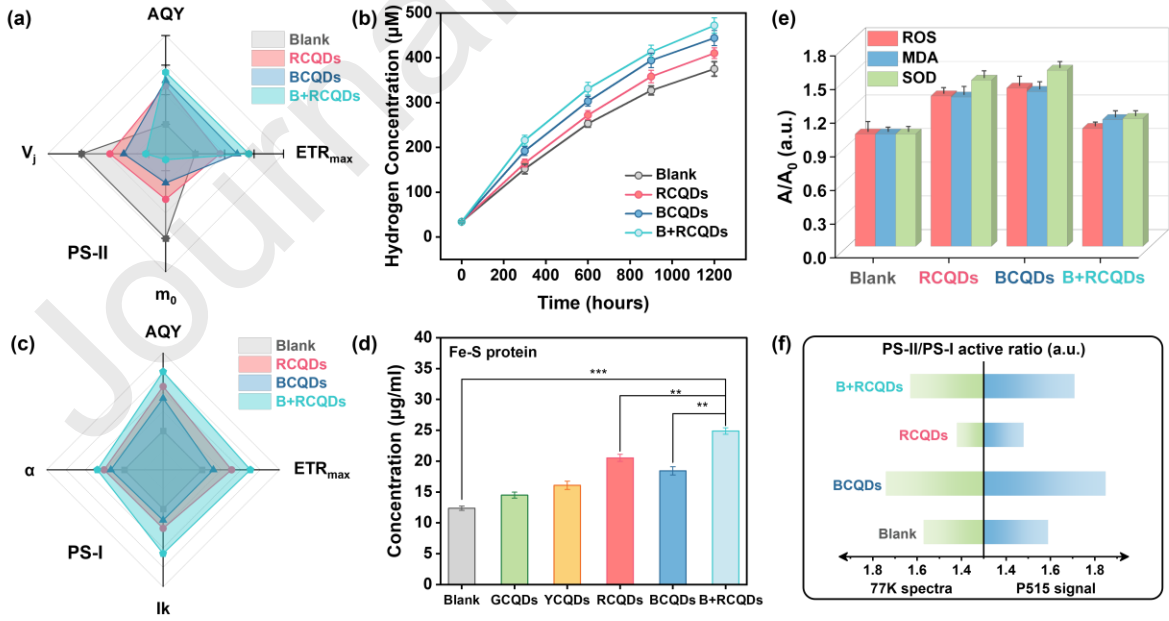

Fig. 5 Intracellular electrons transfer analysis. (a) The time course of oxygen evolution of microalgae with different CQDs (10mg·L^{-1}) cultivation, (b) Corresponding spider plots of chlorophyll fluorescence parameters from aerobic PS-II, (c) Fe-S contents in different biohybrids, 2mL microalgae solution in each test (n=3, P<0.05), (d) Corresponding spider plots of chlorophyll fluorescence parameters from aerobic PS-I, (e) Oxidative stress biomarkers level (P<0.05), and (f) active ratio between PS-I and PS-II in different biohybrids with 77K emission spectra (exciting the sample at 475 nm and recording emission from 500 to 800 nm, normalizing to the GFP signal at 508 nm).

PS-I activity, which significantly impacts the intracellular electron chain, was also measured using various methods. Chlorophyll fluorescence parameters revealed an increase in *ETR* across all biohybrids (**Figure 5c** and **S13**). The rank was enlisted as follow, Blank < GCQD < YCQD < BCQD < RCQD < B+RCQD. Enhanced ETR and other quantum parameters, such as average quantum yield (*AQY*), light capture efficiency (α), and tolerance to light intensity (I_k), verified effective photo-electron energy conversion facilitated by B+RCQDs. The Fe-S proteins, which served as electron carriers in the LEF at PS-I, were found in higher concentrations in the B+RCQDs biohybrid compared to other treatments in **Figure 5d**. Its concentration also positively correlated with LEF efficiency at PS-I and promoting carbon fixation, due to its electron carrying function in the LEF. [65] The generation of Fe-S proteins was stimulated by active nitrogen assimilation and fatty acid synthesis, indicative of efficient microalgal proliferation and ATP/NADPH production. [66] The dual excitation in Chlorophyl a, with its red tropism from P700 excitation, along with the high conductivity of heterojunction nanomaterials, resulted in the most significant PS-I enhancement from composite R- and BCQDs. Comparative analysis of single CQDs indicated that BCQDs were less effective in PS-I activation than RCQDs, contrasting with the activation tendency observed in PS-II. [67] Systematic detection of PS-I confirmed the superior conductivity from B+RCQDs and suggests that RCQDs provide greater assistance to PS-I.

The interplay and connection between PS-I and PS-II require investigation, as imbalanced activity between the two can lead to the generation of excess reactive electrons that may damage microalgae cells. The active electron conductivity from CQDs resulted in higher levels of oxidative stress biomarkers, such as ROS, SOD, and MDA, in all biohybrids. Particularly, a high level of biomarkers and strong photoprotective effect revealed in BCQDs, RCQDs, and B+RCQDs biohybrids, due to active electron transformation (**Figure S14**). The B+RCQDs biohybrid, however, exhibited lower concentrations of oxidative stress biomarkers compared to single CQDs and the control. I t revealed a weaker protective effect and higher carbon fixation efficiency within the intracellular PS. Single PS activation tendency in BCQDs and RCQDs might lead into the imbalanced PS activity and photoprotection. The weak PS-I activity can disrupt the LEF, affecting the redox state of intermediate electron carriers. This excitation could degrade D1 proteins and cell membranes through superoxide radicals and singlet oxygen attack. [68] Moreover, poor PS-II activity can result in over-reduction of PS-I, causing disturbance of the reaction center by ROS. [67] The enhancement tendency observed in RCQDs and BCQDs biohybrids is thus associated

with unbalanced PS activity and oxidative stress, which is harmful for the carbon fixation.

Non-photochemical quenching serves as a photoprotective mechanism to dissipate harmful ROS and free electrons. NPQ indices in PS-II are correlated with self-oxidation from excess electron activation (**Figure S15**). [69] Active NPQ test also emerge excess electron excitations in RCQDs (1.12) and BCQDs (1.24). In contrast, the lower NPQ in B+RCQDs (0.24) approved the lower NPQ in B+RCQDs signifies a higher utilization efficiency of photo-electric energy. Moreover, less quenching also minimized oxidative stress and heat dissipation, these effect both beneficial for microalgae growth and carbon fixation. The enhanced electron carriers in the carbon fixation path also displayed the decreased electron waste in oxidation stress and heat dissipation. [70] Enhanced electron carriers in the LEF, such as ATP/ADP, NADPH/$NADP^+$, and Fe-S proteins, also suggest reduced electron waste in oxidative stress and heat dissipation.

The balance of activity between PS-I and PS-II was directly influenced by the reactive centers in these photosystems. In microalgae cells, the LHC in PS-I and PS-II acted as antennae to capture photo energy for electron excitation and carbon conversion. The ratio of reactive centers in PS-I and PS-II provided evidence of the balance in the photosynthetic system. Gaussian fitting of 77 K fluorescence emission spectra (**Figure 5f** and **S16**) revealed peaks at 685 nm (LHC-II) and 709 nm (LHC-I). [28] Owing to the higher fluorescence intensity at PS-I and II peaks, two PS activation from CQDs could be confirmed from the CQDs activation. Furthermore, the ratio of peaks intensity (I_{685}/I_{709}) in blank, BCQDs, RCQDs and B+RCQDs were calculated as 1.23, 1.45, 1.13 and 1.31, respectively. Owing to the positive correlation between emission intensity and LHC activity, the PS-I and PS-II enhancement tendencies corresponding in RCQD and BCQD biohybrids was confirmed. Moreover, the middle intensity in the B+RCQDs biohybrid represented the balanced two PS activity in the enhancement and the same trend was also confirmed by P515 detection (**Figure S17**). [71] The unbalanced PS-I and II in single CQDs biohybrids generate excess electron in intracellular PS-I or II. Related active products further converse into ROS via cellular respiration, restraining photosynthetic carbon fixation by D1 proteins destruction in chloroplasts and peroxidization at cell membrane. [72] This side effect was mitigated by the composite CQDs, due to balanced activity regulation in both PS-I and PS-II. In summary, B+RCQDs biohybrid optimized PS-I/II enhancement to initiate the synergy of intracellular electrons transfer, activating the intracellular photosynthetic activity for carbon fixation.

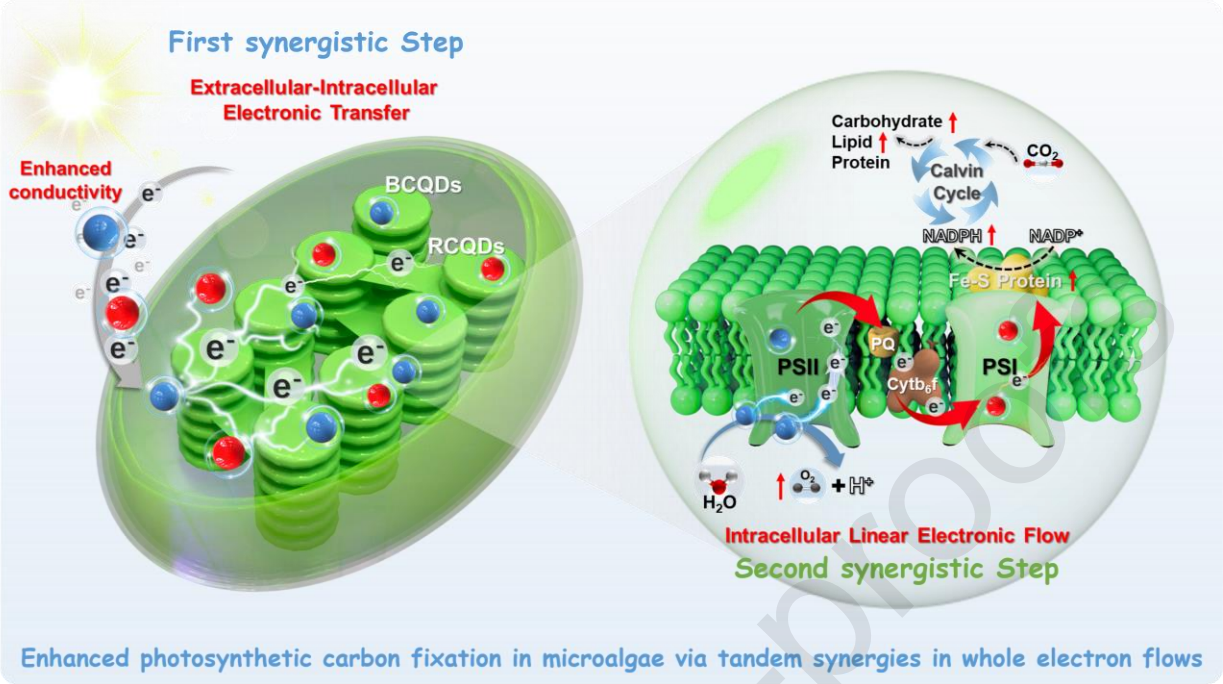

Scheme 1 The mechanism of enhanced photosynthetic carbon fixation in microalgae through tandem synergies from B/R CQDs

Overall, the enhanced microalgal carbon fixation from tandem synergies could be divided into two steps (**Scheme 1**), as following: firstly, the extracellular CQDs assist the extracellular electrons transform into intracellular PS-II. Secondly, the intracellular B/R CQDs optimized the PS-I and II activation for the later LEF and carbon fixation. These tandem synergies work as the dual promotion in the microalgal carbon fixation.

4. Conclusion

Microalgal photosynthesis plays a crucial role in capturing carbon dioxide and converting it into valuable chemicals. However, the limited efficiency of photosynthesis, primarily due to slow electron flow, has hindered the broader application of plant-based carbon fixation. In this study, we address this limitation by incorporating a mixture of red and blue fluorescent carbon quantum dots (CQDs) into microalgal cultivation. These CQDs enhance electron transfer, thereby activating carbon fixation and energy storage. This innovative strategy resulted in a 1.03-fold increase in carbon fixation and a 0.85-fold increase in energy storage. Given the pivotal role of plants in photosynthetic carbon fixation, the enhancement achieved through CQD addition holds significant promise for advancing carbon neutrality and resource recycling.

Mechanistically, our work unveils a cascade synergy in the photosynthetic electron flow. The red and blue fluorescent CQD biohybrids, with their superior conductivity, significantly enhance both extracellular and intracellular electron transfer, thereby boosting photosynthetic carbon fixation. Through integrated photo-electric experiments and intracellular photosynthesis measurements, such as quenching effect analysis, we confirmed that extracellular CQDs facilitate the transfer of extracellular electrons into intracellular PS-II. Further investigation revealed a novel synergistic interplay between intracellular PS-II and PS-I, driven by the dual excitations mediated by CQDs. This synergy significantly enhances photosynthetic activity and LEF. To our knowledge, this is the first study to report such tandem synergies that enhance photosynthetic electron transfer across the entire electron transport chain.

Our findings provide a groundbreaking approach for improving photosynthetic efficiency and offer new insights for fundamental research and engineering applications in carbon neutrality through the integration of functional nanomaterials and photosynthetic plants. However, the potential side effects of CQDs on microalgae and aquatic ecosystems must be carefully considered. Based on the photosynthetic electron flow mechanism and the oxidative stress induced by conductive nanomaterials, future studies should explore nanomaterials-immobilized biofilm carriers to prevent the release of nanomaterials and mitigate potential environmental risks.

Author Contributions

All authors were involved in the discussion and manuscript revision. F. Yi: Conceptualization, Methodology, Data Curation, Formal Analysis, Visualization, Writing - original draft; L. Yang: Methodology, Writing - review & editing, Supervision; L. Zhang: Data Curation, Formal Analysis, Visualization; B. Peng: Formal Analysis, Writing - Review & Editing; X. Tan: Methodology, Formal Analysis; X. You: Methodology, Writing - Review & Editing; Y. Hong: Validation, Formal Analysis; X. Zhou: Funding Acquisition, Supervision; Y. Zhang: Funding Acquisition, Supervision.

Notes

The authors declare no competing financial interest.

Acknowledgments

This work was financially supported by the National Natural Science Foundation of China (No. U21A20322 and 52470034), and Sino-German Cooperation 2.0 Strategic Support Program Project of Tongji University (No. ZD2023002). The authors extend their gratitude to Ms. Li Mengjing from Scientific Compass (www.shiyanjia.com) for providing invaluable assistance with the experiment support of TEM images.

Abbreviations

ATP, Adenosine triphosphate; AQY, Average quantum yield; CBB cycle, Calvin-Benson-Bassham cycle; *C. pyrenoidosa*, *Chlorella pyrenoidosa*; CQDs, Carbon quantum dots; CS_m, Per excited cross-section; EET, Extracellular electron transfer; ETR, Electron transport rate; EY, Eosin Y; HER, Hydrogen evaluation reaction; LEF, Linear electron flow; LHC, Light harvesting complex; m_0, Approximated initial slope (in ms^{-1}) of the fluorescence transient; NPQ, Non-photochemical quenching; P515, Electrochromic shift peak in 515nm; PQ, Plastoquinone; PS-I Photosynthetic system-I; PS-II, Photosynthetic system-II; ROS, Reactive oxygen species; RuBisCo, Ribulose bisphosphate carboxylase oxygenase; TEOA, Triethanolamine; V_j, Relative variable fluorescence at the J – step.

References:

[1] Y. Mao, X. Yang, T.V. Gerven, Amine-Assisted Simultaneous CO2 Absorption and Mineral Carbonation: Effect of Different Categories of Amines, Environmental Science & Technology 57(29) (2023) 10816-10827. https://doi.org/10.1021/acs.est.3c01352.

[2] D.I. Arnon, Conversion of Light into Chemical Energy in Photosynthesis, Nature 184(4679) (1959) 10-21. https://doi.org/10.1038/184010a0.

[3] J.G. Canadell, E.D. Schulze, Global potential of biospheric carbon management for climate mitigation, Nature Communications 5(1) (2014) 5282. https://doi.org/10.1038/ncomms6282.

[4] M.D. Ooms, C.T. Dinh, E.H. Sargent, D. Sinton, Photon management for augmented photosynthesis, Nature Communications 7(1) (2016) 12699. https://doi.org/10.1038/ncomms12699.

[5] M. Sawa, A. Fantuzzi, P. Bombelli, C.J. Howe, K. Hellgardt, P.J. Nixon, Electricity generation from digitally printed cyanobacteria, Nature Communications 8(1) (2017) 1327. https://doi.org/10.1038/s41467-

017-01084-4.

[6] N. Sekar, R.P. Ramasamy, Recent advances in photosynthetic energy conversion, Journal of Photochemistry and Photobiology C: Photochemistry Reviews 22 (2015) 19-33. https://doi.org/https://doi.org/10.1016/j.jphotochemrev.2014.09.004.

[7] Y. Liu, D. Wei, High-efficient CO2-to-protein bioconversion by oleaginous Coccomyxa subellipsoidea using light quality shift and nitrogen supplementation strategy, Chemical Engineering Journal 473 (2023) 145166. https://doi.org/https://doi.org/10.1016/j.cej.2023.145166.

[8] C.Y. Tong, K. Honda, C.J.C. Derek, A review on microalgal-bacterial co-culture: The multifaceted role of beneficial bacteria towards enhancement of microalgal metabolite production, Environmental Research 228 (2023) 115872. https://doi.org/https://doi.org/10.1016/j.envres.2023.115872.

[9] N. Altın, B. Uyar, Increasing power generation and energy efficiency with modified anodes in algae-supported microbial fuel cells, Biomass Conversion and Biorefinery (2025). https://doi.org/10.1007/s13399-025-06536-2.

[10] Z. Chen, Y. Lyu, K. Wang, X. Dong, M. Deng, C. Bai, Y. Xu, W. Zhang, Z. Liu, Preparation of a microalgal photoanode for hydrogen production by photo-bioelectrochemical water-splitting, International Journal of Hydrogen Energy 38(29) (2013) 13045-13049. https://doi.org/https://doi.org/10.1016/j.ijhydene.2013.03.095.

[11] W. Xiong, Y. Peng, W. Ma, X. Xu, Y. Zhao, J. Wu, R. Tang, Microalgae–material hybrid for enhanced photosynthetic energy conversion: a promising path towards carbon neutrality, National Science Review 10(10) (2023). https://doi.org/10.1093/nsr/nwad200.

[12] Y. Weng, X. Bai, M. Kang, Y. Huang, Y. Ji, H. Wang, Z. Hua, Comparative analysis of chemically and green synthesized titanium dioxide nanoparticles for the regulation of photosynthesis in Lactuca sativa L, Environmental Science: Nano 11(1) (2024) 161-174. https://doi.org/10.1039/D3EN00589E.

[13] H. Bernhard Teicher, B. Lindberg Møller, H. Vibe Scheller, Photoinhibition of Photosystem I in field-grown barley (Hordeum vulgare L.): Induction, recovery and acclimation, Photosynthesis Research 64(1) (2000) 53-61. https://doi.org/10.1023/A:1026524302191.

[14] A. Burlacot, Quantifying the roles of algal photosynthetic electron pathways: a milestone towards photosynthetic robustness, New Phytologist 240(6) (2023) 2197-2203. https://doi.org/https://doi.org/10.1111/nph.19328.

[15] S. Zhen, M.W. van Iersel, B. Bugbee, Photosynthesis in sun and shade: the surprising importance of far-red photons, New Phytologist 236(2) (2022) 538-546. https://doi.org/https://doi.org/10.1111/nph.18375.

[16] L. Yang, Q. Su, B. Si, Y. Zhang, Y. Zhang, H. Yang, X. Zhou, Enhancing bioenergy production with carbon capture of microalgae by ultraviolet spectrum conversion via graphene oxide quantum dots, Chemical Engineering Journal 429 (2022) 132230. https://doi.org/https://doi.org/10.1016/j.cej.2021.132230.

[17] H. Jia, Z. Wang, T. Yuan, F. Yuan, X. Li, Y. Li, Z.a. Tan, L. Fan, S. Yang, Electroluminescent Warm White Light-Emitting Diodes Based on Passivation Enabled Bright Red Bandgap Emission Carbon Quantum Dots, Advanced Science 6(13) (2019) 1900397. https://doi.org/https://doi.org/10.1002/advs.201900397.

[18] L.-P. Guo, Y. Zhang, W.-C. Li, Sustainable microalgae for the simultaneous synthesis of carbon quantum dots for cellular imaging and porous carbon for CO2 capture, Journal of Colloid and Interface Science 493 (2017) 257-264. https://doi.org/https://doi.org/10.1016/j.jcis.2017.01.003.

[19] X. Huang, J. Lin, J. Liang, E. Kou, W. Cai, Y. Zheng, H. Zhang, X. Zhang, Y. Liu, W. Li, B. Lei, Pyridinic Nitrogen Doped Carbon Dots Supply Electrons to Improve Photosynthesis and Extracellular Electron Transfer of Chlorella pyrenoidosa, Small 19(31) (2023) 2206222. https://doi.org/https://doi.org/10.1002/smll.202206222.

[20] M. Zhang, H. Wang, Y. Song, H. Huang, M. Shao, Y. Liu, H. Li, Z. Kang, Pristine Carbon Dots Boost the Growth of Chlorella vulgaris by Enhancing Photosynthesis, ACS Applied Bio Materials 1(3) (2018) 894-902. https://doi.org/10.1021/acsabm.8b00319.

[21] S. Wang, Y. Wu, X. Wang, Heterotrophic cultivation of Chlorella pyrenoidosa using sucrose as the sole carbon source by co-culture with Rhodotorula glutinis, Bioresource Technology 220 (2016) 615-620. https://doi.org/https://doi.org/10.1016/j.biortech.2016.09.010.

[22] L. Yang, L. Ren, X. Tan, H. Chu, J. Chen, Y. Zhang, X. Zhou, Removal of ofloxacin with biofuel production by oleaginous microalgae Scenedesmus obliquus, Bioresource Technology 315 (2020) 123738. https://doi.org/https://doi.org/10.1016/j.biortech.2020.123738.

[23] A.E.-F. Abomohra, H. Shang, M. El-Sheekh, H. Eladel, R. Ebaid, S. Wang, Q. Wang, Night illumination using monochromatic light-emitting diodes for enhanced microalgal growth and biodiesel production, Bioresource Technology 288 (2019) 121514. https://doi.org/https://doi.org/10.1016/j.biortech.2019.121514.

[24] F. Yuan, T. Yuan, L. Sui, Z. Wang, Z. Xi, Y. Li, X. Li, L. Fan, Z.a. Tan, A. Chen, M. Jin, S. Yang, Engineering triangular carbon quantum dots with unprecedented narrow bandwidth emission for multicolored LEDs, Nature Communications 9(1) (2018) 2249. https://doi.org/10.1038/s41467-018-04635-5.

[25] B. Sajjadi, W.-Y. Chen, A.A.A. Raman, S. Ibrahim, Microalgae lipid and biomass for biofuel

production: A comprehensive review on lipid enhancement strategies and their effects on fatty acid composition, Renewable and Sustainable Energy Reviews 97 (2018) 200-232. https://doi.org/https://doi.org/10.1016/j.rser.2018.07.050.

[26] J.A. Cruz, C.A. Sacksteder, A. Kanazawa, D.M. Kramer, Contribution of Electric Field ($\Delta\psi$) to Steady-State Transthylakoid Proton Motive Force (pmf) in Vitro and in Vivo. Control of pmf Parsing into $\Delta\psi$ and ΔpH by Ionic Strength, Biochemistry 40(5) (2001) 1226-1237. https://doi.org/10.1021/bi0018741.

[27] S. Viola, B. Bailleul, J. Yu, P. Nixon, J. Sellés, P. Joliot, F.-A. Wollman, Probing the electric field across thylakoid membranes in cyanobacteria, Proceedings of the National Academy of Sciences 116(43) (2019) 21900-21906. https://doi.org/doi:10.1073/pnas.1913099116.

[28] L. Girolomoni, S. Cazzaniga, A. Pinnola, F. Perozeni, M. Ballottari, R. Bassi, LHCSR3 is a nonphotochemical quencher of both photosystems in Chlamydomonas reinhardtii, Proceedings of the National Academy of Sciences 116(10) (2019) 4212-4217. https://doi.org/doi:10.1073/pnas.1809812116.

[29] M.H. Stockett, L. Musbat, C. Kjær, J. Houmøller, Y. Toker, A. Rubio, B.F. Milne, S. Brøndsted Nielsen, The Soret absorption band of isolated chlorophyll a and b tagged with quaternary ammonium ions, Physical Chemistry Chemical Physics 17(39) (2015) 25793-25798. https://doi.org/10.1039/C5CP01513H.

[30] F. Yuan, Z. Wang, X. Li, Y. Li, Z.a. Tan, L. Fan, S. Yang, Bright Multicolor Bandgap Fluorescent Carbon Quantum Dots for Electroluminescent Light-Emitting Diodes, Advanced Materials 29(3) (2017) 1604436. https://doi.org/https://doi.org/10.1002/adma.201604436.

[31] H. Su, Y. Liao, F. Wu, X. Sun, H. Liu, K. Wang, X. Zhu, Cetuximab-conjugated iodine doped carbon dots as a dual fluorescent/CT probe for targeted imaging of lung cancer cells, Colloids and Surfaces B: Biointerfaces 170 (2018) 194-200. https://doi.org/https://doi.org/10.1016/j.colsurfb.2018.06.014.

[32] Q. Zhang, H. Wang, Z. Li, C. Geng, J. Leng, Metal-Free Photocatalyst with Visible-Light-Driven Post-Illumination Catalytic Memory, ACS Applied Materials & Interfaces 9(26) (2017) 21738-21746. https://doi.org/10.1021/acsami.7b02473.

[33] M. Barahoei, M.S. Hatamipour, M. Khosravi, Scaling up the chemical photosynthetic desalination cell by series and parallel arrangements, Desalination 577 (2024) 117420. https://doi.org/https://doi.org/10.1016/j.desal.2024.117420.

[34] F. Chen, N. Yang, X. Huang, J. Lin, H. Zhang, X. Zhang, Y. Liu, W. Li, B. Lei, Carbon dots alleviate photoinhibition and enhance photosynthesis in Chlorella pyrenoidosa, Chemical Engineering Journal 507 (2025) 160429. https://doi.org/https://doi.org/10.1016/j.cej.2025.160429.

[35] X. You, C. Chen, L. Yang, X. Xia, Y. Zhang, X. Zhou, Physiological and morphological responses of

Chlorella pyrenoidosa to different exposure methods of graphene oxide quantum dots, Science of The Total Environment 854 (2023) 158722. https://doi.org/https://doi.org/10.1016/j.scitotenv.2022.158722.

[36] S. Chen, J. Chen, L. Zhang, S. Huang, X. Liu, Y. Yang, T. Luan, S. Zhou, K.H. Nealson, C. Rensing, Biophotoelectrochemical process co-driven by dead microalgae and live bacteria, The ISME Journal 17(5) (2023) 712-719. https://doi.org/10.1038/s41396-023-01383-3.

[37] R. Croce, E. Carmo-Silva, Y.B. Cho, M. Ermakova, J. Harbinson, T. Lawson, A.J. McCormick, K.K. Niyogi, D.R. Ort, D. Patel-Tupper, P. Pesaresi, C. Raines, A.P.M. Weber, X.-G. Zhu, Perspectives on improving photosynthesis to increase crop yield, The Plant Cell 36(10) (2024) 3944-3973. https://doi.org/10.1093/plcell/koae132.

[38] D. Xing, H. Wang, S. Li, C. Jin, Y. Zhao, M. Gao, L. Guo, Insight into the effect of carbon composition on microalgae cultivation using acidogenic fermentation liquid: Growth kinetics, biochemical composition synthesis, and physiological characteristics, Chemical Engineering Journal 488 (2024) 150794. https://doi.org/https://doi.org/10.1016/j.cej.2024.150794.

[39] S.-L. Chen, T.-Y. Wang, C.-C. Tang, R. Wang, Z.-W. He, Z.-H. Li, Y. Tian, X.C. Wang, Revealing mechanisms of triclosan on the removal and distribution of nitrogen and phosphorus in microalgal-bacterial symbiosis system, Environmental Pollution 337 (2023) 122539. https://doi.org/https://doi.org/10.1016/j.envpol.2023.122539.

[40] S. Vellaiyan, An integrated approach for wastewater treatment and algae cultivation: Nutrient removal analysis, biodiesel extraction, and energy and environmental metrics enhancement, Journal of Environmental Management 354 (2024) 120410. https://doi.org/https://doi.org/10.1016/j.jenvman.2024.120410.

[41] C. Wu, W. Xiong, J. Dai, Q. Wu, Genome-Based Metabolic Mapping and 13C Flux Analysis Reveal Systematic Properties of an Oleaginous Microalga Chlorella protothecoides Plant Physiology 167(2) (2014) 586-599. https://doi.org/10.1104/pp.114.250688.

[42] H. Treves, A. Küken, S. Arrivault, H. Ishihara, I. Hoppe, A. Erban, M. Höhne, T.A. Moraes, J. Kopka, J. Szymanski, Z. Nikoloski, M. Stitt, Carbon flux through photosynthesis and central carbon metabolism show distinct patterns between algae, C3 and C4 plants, Nature Plants 8(1) (2022) 78-91. https://doi.org/10.1038/s41477-021-01042-5.

[43] Y. Mao, K. Ye, S. Yang, M. Salam, W. Yu, Q. He, R. He, H. Li, Repeated Exposure Enhanced Toxicity of Clarithromycin on Microcystis aeruginosa Versus Single Exposure through Photosynthesis, Oxidative Stress, and Energy Metabolism Shift, Environmental Science & Technology 58(9) (2024) 4070-4082. https://doi.org/10.1021/acs.est.3c07008.

[44] M. Baba, F. Kikuta, I. Suzuki, M.M. Watanabe, Y. Shiraiwa, Wavelength specificity of growth,

photosynthesis, and hydrocarbon production in the oil-producing green alga Botryococcus braunii, Bioresource Technology 109 (2012) 266-270. https://doi.org/https://doi.org/10.1016/j.biortech.2011.05.059.

[45] N. Atkinson, R. Stringer, S.R. Mitchell, D. Seung, A.J. McCormick, SAGA1 and SAGA2 promote starch formation around proto-pyrenoids in Arabidopsis chloroplasts, Proceedings of the National Academy of Sciences 121(4) (2024) e2311013121. https://doi.org/doi:10.1073/pnas.2311013121.

[46] C. Fei, A.T. Wilson, N.M. Mangan, N.S. Wingreen, M.C. Jonikas, Modelling the pyrenoid-based CO2-concentrating mechanism provides insights into its operating principles and a roadmap for its engineering into crops, Nature Plants 8(5) (2022) 583-595. https://doi.org/10.1038/s41477-022-01153-7.

[47] A. Krishnan, G.K. Kumaraswamy, D.J. Vinyard, H. Gu, G. Ananyev, M.C. Posewitz, G.C. Dismukes, Metabolic and photosynthetic consequences of blocking starch biosynthesis in the green alga hlamydomonas reinhardtii sta6 mutant, The Plant Journal 81(6) (2015) 947-960. https://doi.org/https://doi.org/10.1111/tpj.12783.

[48] X. Zhu, Z. Xu, H. Tang, L. Nie, R. Nie, R. Wang, X. Liu, X. Huang, Photosynthesis-Mediated Intracellular Biomineralization of Gold Nanoparticles inside Chlorella Cells towards Hydrogen Boosting under Green Light, Angewandte Chemie International Edition 62(33) (2023) e202308437. https://doi.org/https://doi.org/10.1002/anie.202308437.

[49] X. Zhou, Y. Zeng, Y. Tang, Y. Huang, F. Lv, L. Liu, S. Wang, Artificial regulation of state transition for augmenting plant photosynthesis using synthetic light-harvesting polymer materials, Science Advances 6(35) (2020) eabc5237. https://doi.org/doi:10.1126/sciadv.abc5237.

[50] R. Xue, L. Fu, S. Dong, H. Yang, D. Zhou, Promoting Chlorella photosynthesis and bioresource production using directionally prepared carbon dots with tunable emission, Journal of Colloid and Interface Science 569 (2020) 195-203. https://doi.org/https://doi.org/10.1016/j.jcis.2020.02.080.

[51] C.M. Lewis, J.D. Flory, T.A. Moore, A.L. Moore, B.E. Rittmann, W.F.J. Vermaas, C.I. Torres, P. Fromme, Electrochemically Driven Photosynthetic Electron Transport in Cyanobacteria Lacking Photosystem II, Journal of the American Chemical Society 144(7) (2022) 2933-2942. https://doi.org/10.1021/jacs.1c09291.

[52] S. Wilson, M.P. Johnson, A.V. Ruban, Proton motive force in plant photosynthesis dominated by ΔpH in both low and high light, Plant Physiology 187(1) (2021) 263-275. https://doi.org/10.1093/plphys/kiab270.

[53] H. Wang, L. Hu, H. Li, Y.-T. Lai, X. Wei, X. Xu, Z. Cao, H. Cao, Q. Wan, Y.-Y. Chang, A. Xu, Q. Zhou, G. Jiang, M.-L. He, H. Sun, Mitochondrial ATP synthase as a direct molecular target of chromium(III) to ameliorate hyperglycaemia stress, Nature Communications 14(1) (2023) 1738. https://doi.org/10.1038/s41467-023-37351-w.

[54] J.R. Evans, Acclimation by the thylakoid membranes to growth irradiance and the partitioning of nitrogen between soluble and thylakoid proteins, Australian Journal of Plant Physiology 15 (1988) 93-106.

[55] M. López-Ortiz, R.A. Zamora, M.I. Giannotti, C. Hu, R. Croce, P. Gorostiza, Distance and Potential Dependence of Charge Transport Through the Reaction Center of Individual Photosynthetic Complexes, Small 18(7) (2022) 2104366. https://doi.org/https://doi.org/10.1002/smll.202104366.

[56] X. Zhou, P. Gai, P. Zhang, H. Sun, F. Lv, L. Liu, S. Wang, Conjugated Polymer Enhanced Photoelectric Response of Self-Circulating Photosynthetic Bioelectrochemical Cell, ACS Applied Materials & Interfaces 11(42) (2019) 38993-39000. https://doi.org/10.1021/acsami.9b12560.

[57] S. Zhang, Y. Wu, L. Zhou, N.A. Al-Dhabi, S. Sun, J. Cai, T. Li, H. Wu, F. Li, W. Tang, Electrode potential regulates extracellular polymer secretion enhanced tetracycline removal, Chemical Engineering Journal 485 (2024) 149942. https://doi.org/https://doi.org/10.1016/j.cej.2024.149942.

[58] S.T. Stripp, T. Happe, How algae produce hydrogen—news from the photosynthetic hydrogenase, Dalton Transactions (45) (2009) 9960-9969. https://doi.org/10.1039/B916246A.

[59] Y. Wu, X. Zhu, X. Wang, Z. Lin, J.R. Reinfelder, F. Li, T. Liu, A New Electron Shuttling Pathway Mediated by Lipophilic Phenoxazine via the Interaction with Periplasmic and Inner Membrane Proteins of Shewanella oneidensis MR-1, Environmental Science & Technology 57(6) (2023) 2636-2646. https://doi.org/10.1021/acs.est.2c07862.

[60] Y. Xu, B.-Y. Peng, X. Zhang, Q. Xu, L. Yang, J. Chen, X. Zhou, Y. Zhang, The aging of microplastics exacerbates the damage to photosynthetic performance and bioenergy production in microalgae (Chlorella pyrenoidosa), Water Research 259 (2024) 121841. https://doi.org/https://doi.org/10.1016/j.watres.2024.121841.

[61] Z. Xu, J. Qi, S. Wang, X. Liu, M. Li, S. Mann, X. Huang, Algal cell bionics as a step towards photosynthesis-independent hydrogen production, Nature Communications 14(1) (2023) 1872. https://doi.org/10.1038/s41467-023-37608-4.

[62] W. Wasilewska-Dębowska, M. Galas, P. Rogowski, J. Trojanowska, A. Urban, D. Charnyak, A. Levytska, E. Romanowska, The NDH complex can be involved in the regulation of phosphorylation of LHCII proteins and tolerance of Echinochloa crus-galli (L.) to high light intensity, Environmental and Experimental Botany 220 (2024) 105680. https://doi.org/https://doi.org/10.1016/j.envexpbot.2024.105680.

[63] B. Wang, M. Ma, H. Lu, Q. Meng, G. Li, X. Yang, Photosynthesis, sucrose metabolism, and starch accumulation in two NILs of winter wheat, Photosynthesis Research 126(2) (2015) 363-373. https://doi.org/10.1007/s11120-015-0126-9.

[64] K. Akiyama, S.-I. Ozawa, Y. Takahashi, K. Yoshida, T. Suzuki, K. Kondo, K.-i. Wakabayashi, T.

Hisabori, Two specific domains of the γ subunit of chloroplast FoF1 provide redox regulation of the ATP synthesis through conformational changes, Proceedings of the National Academy of Sciences 120(6) (2023) e2218187120. https://doi.org/doi:10.1073/pnas.2218187120.

[65] Y. Sun, L. Jiang, S. Gong, G. Diaz-Pulido, X. Yuan, H. Tong, L. Huang, G. Zhou, Y. Zhang, H. Huang, Changes in physiological performance and protein expression in the larvae of the coral Pocillopora damicornis and their symbionts in response to elevated temperature and acidification, Science of The Total Environment 807 (2022) 151251. https://doi.org/https://doi.org/10.1016/j.scitotenv.2021.151251.

[66] H. Ye, M. Pilon, E.A.H. Pilon-Smits, CpNifS-dependent iron-sulfur cluster biogenesis in chloroplasts, New Phytologist 171(2) (2006) 285-292. https://doi.org/https://doi.org/10.1111/j.1469-8137.2006.01751.x.

[67] P. Bag, T. Shutova, D. Shevela, J. Lihavainen, S. Nanda, A.G. Ivanov, J. Messinger, S. Jansson, Flavodiiron-mediated O2 photoreduction at photosystem I acceptor-side provides photoprotection to conifer thylakoids in early spring, Nature Communications 14(1) (2023) 3210. https://doi.org/10.1038/s41467-023-38938-z.

[68] A. Kumar, A. Prasad, M. Sedlářová, R. Kale, L.K. Frankel, L. Sallans, T.M. Bricker, P. Pospíšil, Tocopherol controls D1 amino acid oxidation by oxygen radicals in Photosystem II, Proceedings of the National Academy of Sciences 118(4) (2021) e2019246118. https://doi.org/doi:10.1073/pnas.2019246118.

[69] X. Zhang, X. Hu, H. Wu, L. Mu, Persistence and Recovery of ZIF-8 and ZIF-67 Phytotoxicity, Environmental Science & Technology 55(22) (2021) 15301-15312. https://doi.org/10.1021/acs.est.1c05838.

[70] B. Karpinska, C.H. Foyer, Superoxide signalling and antioxidant processing in the plant nucleus, Journal of Experimental Botany 75(15) (2024) 4599-4610. https://doi.org/10.1093/jxb/erae090.

[71] P. Joliot, A. Joliot, In Vivo Analysis of the Electron Transfer within Photosystem I: Are the Two Phylloquinones Involved?, Biochemistry 38(34) (1999) 11130-11136. https://doi.org/10.1021/bi990857c.

[72] H. Xu, L.a. Li, Y. Wang, K. Qiu, S. Chen, J. Zeng, R. Liu, Q. Yang, W. Huang, Differential physiological response of marine and freshwater microalgae to polystyrene microplastics, Journal of Hazardous Materials 448 (2023) 130814. https://doi.org/https://doi.org/10.1016/j.jhazmat.2023.130814.

Highlights

- Dual fluorescent CQDs were more efficient to activate microalgal carbon fixation.
- Electron activation in microalgae was confirmed in photosynthetic electron flow.
- It is the first proof of tandem synergies in the whole photosynthetic electron flow.

Graphic Abstract:

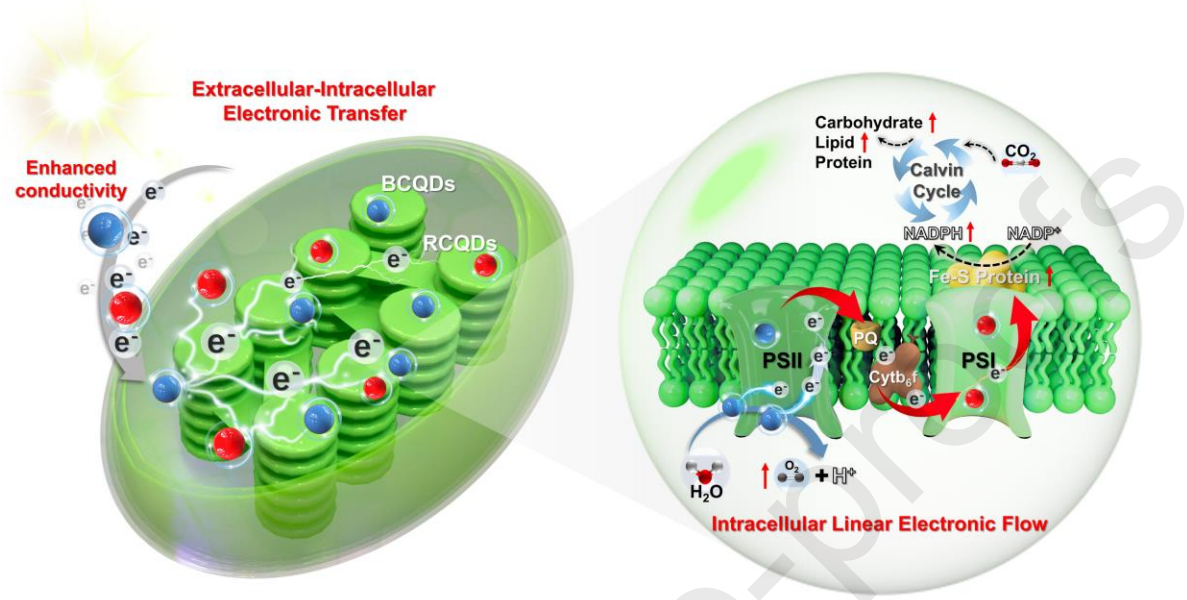

Blue and red florescent carbon quantum dots activated microalgal cultivation and carbon fixation via in electron transport flows.